

FREQUENCY-UNDERSAMPLED SHORT-TIME FOURIER TRANSFORM

Daichi Kitahara

College of Information Science and Engineering, Ritsumeikan University, Shiga, Japan

ABSTRACT

The short-time Fourier transform (STFT) usually computes the same number of frequency components as the frame length while overlapping adjacent time frames by more than half. As a result, the number of components of a *spectrogram matrix* becomes more than twice the signal length, and hence STFT is hardly used for signal compression. In addition, even if we modify the spectrogram into a desired one by spectrogram-based signal processing, it is re-changed during the inversion as long as it is outside the range of STFT. In this paper, to reduce the number of components of a spectrogram while maintaining the analytical ability, we propose the *frequency-undersampled STFT (FUSTFT)*, which computes only half the frequency components. We also present the inversions with and without the *periodic condition*, including their different properties. In simple numerical examples of audio signals, we confirm the validity of FUSTFT and the inversions.

Index Terms—Short-time Fourier transform, redundancy, spectrogram, inversions with and without periodicity, tridiagonal system.

1. INTRODUCTION

Time-frequency analysis is to capture the temporal variations of frequency components of a target signal [1]–[18]. In audio signal processing, the short-time Fourier transform (STFT) [1]–[9] is the most commonly used time-frequency analysis method since STFT inherits the robustness, of the Fourier transform, against time shifts [10]. The result of STFT is called a *spectrogram*, and it is often expressed as a matrix. In addition to using spectrograms for signal analysis and feature extraction, we can also generate desired time-domain signals through modification of the spectrograms themselves [19]–[26]. This paper is particularly aware of the latter usage of the spectrograms.

In most cases of the engineering field, STFT is used for discrete-time signals, and a window function has a compact support. In such a case, the support length of the discrete-time window function, called the *window length*, is directly equal to the length of each time frame, called the *frame length*. Typically, we calculate the same number of frequency components as the frame length in each time frame by using the fast Fourier transform (FFT). We call this the *discrete STFT*.

We can also compute more frequency components, although that are *linearly dependent*, in each time frame by padding zeros before FFT. We call this the *frequency-oversampled STFT (FOSTFT)*. Both the discrete STFT and FOSTFT are also called the *windowed discrete Fourier transform (WDFT)* or the *discrete Gabor transform (DGT)*, but in this paper we switch the names by focusing on the inequality between the frame length and the number of frequency components.

The inversions, based on the *Moore–Penrose pseudoinverse*, for the discrete STFT and FOSTFT can be easily computed by using the so-called *canonical dual window* [27], [28], whose window length is the same as the frame length, after the inverse FFT (IFFT). These inversions for the discrete STFT and FOSTFT are called *painless* [29].

From the facts that (i) human hearing is sensitive to block boundary artifacts and (ii) a window function makes signal values small at

both ends of each time frame, we usually overlap adjacent frames by more than half in the computation of the discrete STFT and FOSTFT. As a result, the number of components of a spectrogram matrix becomes more than twice the original signal length, and hence the spectrogram is hardly used for signal compression. Moreover, even if we set components of a spectrogram to desired values by a spectrogram-based signal processing technique such as [19]–[26], there is a risk that both magnitudes and phases would be greatly changed during the inversion unless the desired spectrogram belongs to the range of STFT.

As *almost nonredundant* time-frequency analysis methods,¹ the *modified discrete cosine transform (MDCT)* [11], that is used in coding formats for audio signals such as MP3 and AAC, and the *discrete Wilson transform (DWT)* [12], [13], that is hardly used in an application because of a strict condition for a window function, are known. The results of the discrete STFT and FOSTFT are complex-valued, while those of MDCT and DWT are real-valued and unsuitable for analysis of complex-valued signals. Moreover, MDCT and DWT are sensitive to time shifts differently from STFT. As a complex version of MDCT, the *modulated complex lapped transform (MCLT)* [14] is known but it is almost the same as the discrete STFT (see Footnote 8).

In this paper, to suppress the redundancy of a spectrogram while maintaining the original analytical ability, we propose the *frequency-undersampled STFT (FUSTFT)*, which calculates only half the frequency components of the discrete STFT in each time frame. From the fact that the energy of a target signal spreads along the frequency axis by multiplying a smooth window function, FUSTFT maintains the features of the original spectrogram of the discrete STFT despite the undersampling. In fact, Stanković has already proposed the special case of FUSTFT in [30], that is equivalent to Type-I FUSTFT in (11) with $\xi = \frac{L_w}{2}$.² Hence, this paper is the generalization of [30].

By using FUSTFT, we can easily obtain efficient spectrograms, including almost nonredundant ones, while its inversion is not so simple differently from those for the discrete STFT and FOSTFT, i.e., its inversion process changes dependently on the signal length [31]. We realize the inversions with and without the *periodic condition*, which is assumed in [6]–[8], by directly solving the least squares problems. In [31] the general frequency-undersampling is considered while this paper treats only the half frequency-undersampling and clarifies that both two different inversions can always be computed very quickly.

2. DEFINITIONS OF STFT AND ISTFT IN THIS PAPER

Let \mathbb{R} and \mathbb{C} be the sets of all real numbers and all complex numbers, respectively. The imaginary unit is denoted by $i \in \mathbb{C}$, i.e., $i^2 = -1$. We write vectors and matrices with boldface small and capital letters, respectively. We express the transpose operator as $(\cdot)^T$ and the adjoint operator as $(\cdot)^H$. We express the composition of mappings as \circ and the inverse of a nonsingular matrix by $(\cdot)^{-1}$. We express the ℓ_2 norm of a vector as $\|\cdot\|_2$ and the Frobenius norm of a matrix as $\|\cdot\|_F$. The floor and ceiling functions are denoted by $\lfloor \cdot \rfloor$ and $\lceil \cdot \rceil$, respectively. For $a > 0$, we define $\text{mod}_a : \mathbb{R} \rightarrow [0, a)$ by $\text{mod}_a(b) := b - \lfloor \frac{b}{a} \rfloor a$.

This work was supported in part by JSPS Grants-in-Aid Grant Number for Early-Career Scientists JP19K20361 (e-mail: d-kita@fc.ritsumei.ac.jp).

¹The redundancies of MDCT and DWT occur at the first and last frames.

²Strictly speaking, sampling points of a window function are also changed.

2.1. Continuous-Time / Discrete-Time / Discrete STFT

Let $x : \mathbb{R} \rightarrow \mathbb{C}$ be a real-valued or complex-valued continuous-time signal. In this paper, with a real-valued window function $w : \mathbb{R} \rightarrow \mathbb{R}$, we define the *continuous-time STFT* of $x(t)$ by³

$$X(f, t) = \int_{-\infty}^{\infty} x(\tau) w(\tau - t) e^{-i2\pi f(\tau - t - \frac{T_s}{2})} d\tau \quad (1)$$

and the *discrete-time STFT* by⁴

$$\begin{aligned} X_d(f, t) &= \sum_{\tau=-\infty}^{\infty} x(\tau T_s) w(\tau T_s - t) e^{-i2\pi f(\tau T_s - t - \frac{T_s}{2})} \\ &= \frac{1}{T_s} \sum_{\kappa=-\infty}^{\infty} X(f - \kappa f_s, t), \end{aligned} \quad (2)$$

where $f \in \mathbb{R}$, $t \in \mathbb{R}$, $T_s > 0$ is the sampling interval of a discrete-time signal $x[\tau] := x(\tau T_s)$, and $f_s = \frac{1}{T_s}$ is the sampling frequency. From (3), $X_d(f, t)$ is periodic on f with period f_s , and hence we can restrict f to $f \in [-\frac{f_s}{2}, \frac{f_s}{2})$ or $f \in [0, f_s)$ in the discrete-time STFT.

In what follows, let $L_w (\geq 2)$ be an integer, and we suppose that the window function $w(t)$ has a compact support of length $L_w T_s$, i.e., $w(t) \neq 0$ for almost all $t \in (0, L_w T_s)$ and $w(t) = 0$ otherwise, and $w(t)$ is a symmetric curve, i.e., $w(\frac{L_w T_s}{2} - t) = w(\frac{L_w T_s}{2} + t)$ for all $t \in \mathbb{R}$ and $w'(t) \neq 0$ for almost all $t \in (0, L_w T_s)$. Under these assumptions,⁵ the continuous-time STFT in (1) is expressed as

$$X(f, t) = \int_0^{L_w T_s} x(\tau + t) w(\tau) e^{-i2\pi f(\tau - \frac{T_s}{2})} d\tau. \quad (4)$$

In (2), we can define the discrete-time STFT for all $t \in \mathbb{R}$, but there is almost no need to calculate $X_d(f, t)$ at intervals shorter than T_s . Let l be the time frame index. With an integer frame shift $\xi (\leq L_w)$, we discretize the time t of $X_d(f, t)$ by $t = (l\xi - L_w + \xi - \frac{1}{2})T_s$, i.e.,

$$X_d(f, (l\xi - L_w + \xi - \frac{1}{2})T_s) = \sum_{\tau=0}^{L_w-1} x[\tau + l\xi - L_w + \xi] w[\tau] e^{-i2\pi f \tau T_s}, \quad (5)$$

where $f \in [0, f_s)$ and $w[\tau] := w((\tau + \frac{1}{2})T_s) \neq 0$. Next, let k be the frequency index, and discretize the frequency f in (5) by $f = \frac{k}{L_w} f_s$ since the maximum number of *independent* frequency components computed in each time frame is L_w . For a discrete-time signal $\mathbf{x} := (x[0], x[1], \dots, x[L_x - 1])^T \in \mathbb{C}^{L_x}$ of length $L_x (> L_w)$, we define

$$\begin{aligned} \text{STFT}(\mathbf{x})[k, l] &= X_d(\frac{k}{L_w} f_s, (l\xi - L_w + \xi - \frac{1}{2})T_s) \\ &= \sum_{\tau=0}^{L_w-1} x[\tau + l\xi - L_w + \xi] w[\tau] e^{-i2\pi \frac{k}{L_w} \tau} \end{aligned} \quad (6)$$

as the *discrete STFT* in this paper,⁶ where $k = 0, 1, \dots, L_w - 1$ and

³We use the sampling interval T_s in the definition of the continuous-time STFT so that a discrete-time window function $w[\tau]$ in (5) will be symmetric.

⁴Note that we can define $X_d(f, t)$ for all $t \in \mathbb{R}$ regardless of T_s because the window function and the complex sinusoid are computable for any time t .

⁵The rectangular window is out of the discussion because it is not a curve.

⁶For *phase-aware* signal processing, it is shown in [10] that another STFT

$$X(f, t) = \int_0^{L_w T_s} x(\tau + t) w(\tau) e^{-i2\pi f(\tau + t)} d\tau \quad (7)$$

is better than (4) since complex spectrograms based on (7) will be lower rank. If we use two or more spectrograms with window functions of *different* L_w , it is better to change the support of $w(t)$ into $(-\frac{L_w T_s}{2}, \frac{L_w T_s}{2})$ and compute

$$X(f, t) = \int_{-\frac{L_w T_s}{2}}^{\frac{L_w T_s}{2}} x(\tau + t) w(\tau) e^{-i2\pi f(\tau + t)} d\tau \quad (8)$$

instead of (7) since (8) aligns time frames of *different* lengths at their centers.

$l = 0, 1, \dots, \lceil \frac{L_x + L_w - 2\xi}{\xi} \rceil$. In (6), by assuming that $x(t) = 0$ for all $t \in (-\infty, -\frac{T_s}{2}] \cup [(L_x - \frac{1}{2})T_s, \infty)$, we padded $L_w - \xi$ zeros at the beginning of \mathbf{x} and $\lceil \frac{L_x + L_w - \xi}{\xi} \rceil \xi - L_x$ zeros at the end. The discrete STFT in (6) is easily computed by FFT after multiplying the window function $w[\tau]$ and extracted time frame signals of length L_w . Unless L_w is too large or ξ is too small, a complex spectrogram $\text{STFT}(\mathbf{x}) = (\text{STFT}(\mathbf{x})[k, l]) \in \mathbb{C}^{L_w \times \lceil \frac{L_x + L_w - \xi}{\xi} \rceil}$ can be quickly obtained [31].

In each time frame, we can also compute more frequency components than L_w , that are *linearly dependent*. We call this transform the *frequency-oversampled STFT (FOSTFT)*. Specifically, let N_z be a positive integer, discretize f in (5) by $f = \frac{k}{L_w + N_z} f_s$, and we define

$$\begin{aligned} \text{FOSTFT}(\mathbf{x})[k, l] &= X_d(\frac{k}{L_w + N_z} f_s, (l\xi - L_w + \xi - \frac{1}{2})T_s) \\ &= \sum_{\tau=0}^{L_w-1} x[\tau + l\xi - L_w + \xi] w[\tau] e^{-i2\pi \frac{k}{L_w + N_z} \tau}, \end{aligned} \quad (9)$$

where $k = 0, 1, \dots, L_w + N_z - 1$ and $l = 0, 1, \dots, \lceil \frac{L_x + L_w - 2\xi}{\xi} \rceil$. FOSTFT in (9) is computed by padding N_z zeros right before FFT.

2.2. Inversions for the Discrete STFT and FOSTFT

The discrete STFT in (6) is a *linear mapping* and we express its *range* as $\mathcal{R} := \{\mathbf{X} \in \mathbb{C}^{L_w \times \lceil \frac{L_x + L_w - \xi}{\xi} \rceil} \mid \exists \mathbf{x} \in \mathbb{C}^{L_x} \mathbf{X} = \text{STFT}(\mathbf{x})\}$. As long as $\xi < L_w$, the discrete STFT is *redundant*, and there are innumerable linear mappings that recover, from a complex spectrogram $\mathbf{X} \in \mathcal{R}$, the corresponding signal \mathbf{x} [27]. To recover the most consistent signal \mathbf{x} from $\mathbf{X} \notin \mathcal{R}$, we define the *inverse STFT (ISTFT)* by

$$\text{ISTFT}(\mathbf{X}) = \underset{\mathbf{x} \in \mathbb{C}^{L_x}}{\text{argmin}} \|\mathbf{X} - \text{STFT}(\mathbf{x})\|_F^2. \quad (10)$$

We express the discrete STFT as $\mathcal{S} : \mathbb{C}^{L_x} \rightarrow \mathbb{C}^{L_w \times \lceil \frac{L_x + L_w - \xi}{\xi} \rceil}$. Then, since ISTFT in (10) is the *Moore–Penrose pseudoinverse* of \mathcal{S} , we have $\text{ISTFT}(\mathbf{X}) = (\mathcal{S}^H \circ \mathcal{S})^{-1} \circ \mathcal{S}^H(\mathbf{X})$. The matrix $\mathcal{S}^H \circ \mathcal{S} \in \mathbb{R}^{L_w \times L_w}$ is diagonal, and its diagonal components are periodic with period ξ . Hence, ISTFT can be quickly computed by using IFFT and the pre-designed *canonical dual window* [27]. For FOSTFT in (9) we can compute its inversion by using the same canonical dual window.

3. FREQUENCY-UNDERSAMPLED STFT

It is known that human hearing is sensitive to block boundary artifacts [11]. Moreover, in each time frame, a non-rectangular window $w[\tau]$ makes signal values at both ends very small. From these facts, we usually restrict the frame shift ξ to $\xi \leq \frac{L_w}{2}$ in (6) and (9). However, in this usual case, the number of components of a spectrogram matrix is more than twice the signal length L_x , which is not suitable for signal compression. In addition, even if we obtain desired spectrograms through spectrogram-based signal processing, their components will be changed by ISTFT unless they belong to the range \mathcal{R} .

In what follows, L_w is a *multiple of 4*. For more efficient time-frequency analysis, we propose the *frequency-undersampled STFT (FUSTFT)*, that computes $\frac{L_w}{2}$ frequency components in each frame. We discretize f in (5) by $f = \frac{2k}{L_w} f_s$, and define *Type-I FUSTFT* as

$$\begin{aligned} \text{FUSTFT}_I(\mathbf{x})[k, l] &= X_d(\frac{2k}{L_w} f_s, (l\xi - L_w + \xi - \frac{1}{2})T_s) \\ &= \sum_{\tau=0}^{L_w-1} x[\tau + l\xi - L_w + \xi] w[\tau] e^{-i2\pi \frac{2k}{L_w} \tau}. \end{aligned} \quad (11)$$

Discretize f in (5) by $f = \frac{2k+1}{L_w} f_s$, and define *Type-II FUSTFT* as

$$\begin{aligned} \text{FUSTFT}_{II}(\mathbf{x})[k, l] &= X_d(\frac{2k+1}{L_w} f_s, (l\xi - L_w + \xi - \frac{1}{2})T_s) \\ &= \sum_{\tau=0}^{L_w-1} x[\tau + l\xi - L_w + \xi] w[\tau] e^{-i2\pi \frac{2k+1}{L_w} \tau}. \end{aligned} \quad (12)$$

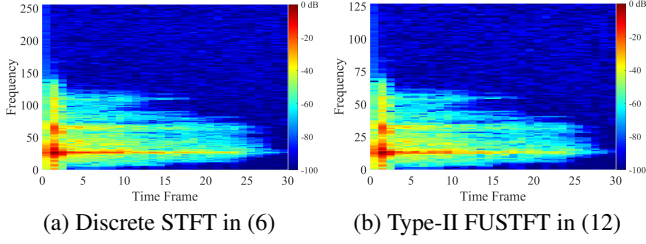


Fig. 1. Power spectrograms of a clicking sound of 0.2 seconds [32].

By using Type-I and Type-II alternately, define *Type-III FUSTFT* as $\text{FUSTFT}_{\text{III}}(\mathbf{x})[k, l]$

$$= \begin{cases} \sum_{\tau=0}^{L_w-1} x[\tau + l\xi - L_w + \xi] w[\tau] e^{-i2\pi \frac{2k}{L_w} \tau} & \text{if } l \text{ is even,} \\ \sum_{\tau=0}^{L_w-1} x[\tau + l\xi - L_w + \xi] w[\tau] e^{-i2\pi \frac{2k+1}{L_w} \tau} & \text{if } l \text{ is odd.} \end{cases} \quad (13)$$

From (11) to (13), $k = 0, 1, \dots, \frac{L_w}{2} - 1, l = 0, 1, \dots, \lceil \frac{L_x + L_w - 2\xi}{\xi} \rceil$, and $\xi \leq \frac{L_w}{2}$. As shown in Fig. 1,⁷ the number of frequency bins of FUSTFT is half of that of the discrete STFT.⁸ Since the energy of \mathbf{x} spreads along the frequency axis by multiplying a window function, FUSTFT maintains the characteristics of the standard spectrogram of the discrete STFT despite undersampling of frequency components.

4. TWO DIFFERENT INVERSIONS FOR FUSTFT

4.1. Inversion Based on the Standard Pseudoinverse

Differently from cases of the discrete STFT and FOSTFT, the inversion for FUSTFT is not simple, i.e., the canonical dual window *does not exist* and the computation process changes dependently on L_x . In this paper, we realize the inversion by solving the problem similar to (10). Let $\mathcal{S} : \mathbb{C}^{L_x} \rightarrow \mathbb{C}^{\frac{L_w}{2} \times \lceil \frac{L_x + L_w - \xi}{\xi} \rceil}$ be one of the linear mappings (11), (12), and (13). Then the inversion based on the pseudoinverse is expressed as $(\mathcal{S}^H \circ \mathcal{S})^{-1} \circ \mathcal{S}^H$. In FUSTFT cases, $\mathcal{S}^H \circ \mathcal{S}$ is

$$\begin{bmatrix} a_0 & & b_0 & & & \\ & a_1 & & b_1 & & \\ & & \ddots & & \ddots & \\ b_0 & & a_{\frac{L_w}{2}} & & b_{\frac{L_w}{2}} & \\ & b_1 & & a_{\frac{L_w}{2}+1} & & \\ & & \ddots & & \ddots & \\ & & b_{\frac{L_w}{2}} & & a_{L_x - \frac{L_w}{2} - 1} & b_{L_x - \frac{L_w}{2} - 1} \\ & & & \ddots & & \\ & & & & a_{L_x - 1} & \\ & & & & & b_{L_x - \frac{L_w}{2} - 1} \end{bmatrix}. \quad (15)$$

⁷In Fig. 1, $f_s = 44,100$ [Hz], $L_w = 512$, $\xi = \frac{L_w}{2} = 256$, and we used the normalized sine window $w[\tau] := \frac{1}{\sqrt{L_w}} \sin(\frac{1}{L_w}(\tau + \frac{1}{2})\pi)$ for both (6) and (12). Since a sound \mathbf{x} is real-valued, one in each complex conjugate pair, e.g., $\text{FUSTFT}_{\text{II}}(\mathbf{x})[k, l]$ and $\text{FUSTFT}_{\text{II}}(\mathbf{x})[\frac{L_w}{2} - k - 1, l]$, was omitted.

⁸Combining FOSTFT of $N_z = L_w$ and Type-II FUSTFT, we can *redefine*

$$\text{STFT}(\mathbf{x})[k, l] = \sum_{\tau=0}^{L_w-1} x[\tau + l\xi - L_w + \xi] w[\tau] e^{-i2\pi \frac{2k+1}{2L_w} \tau} \quad (14)$$

as the discrete STFT. If we express the transform in (14) as a linear mapping \mathcal{S} , its inversion is easily computed since $\mathcal{S}^H \circ \mathcal{S}$ is the same as (6). (14) with $\xi = \frac{L_w}{2}$ and MCLT [14] have the *same magnitudes* and differ only in phases.

In (15),⁹ diagonal components are

$$a_i = \frac{L_w}{2} \sum_{l=0}^{\lceil \frac{L_w}{\xi} \rceil - 1} w^2[m_i + l\xi] \quad (16)$$

for all the three types, where $m_i = \text{mod}_{\xi}(i + L_w)$ and $w[\tau] = 0$ for $\tau \geq L_w$. For Type-I FUSTFT, nonzero nondiagonal components are

$$b_i = \frac{L_w}{2} \sum_{l=0}^{\lceil \frac{L_w}{2\xi} \rceil - 1} w[m_i + l\xi] w[m_i + l\xi + \frac{L_w}{2}]. \quad (17)$$

For Type-II, each b_i is equal to (17) multiplied by -1 . For Type-III,

$$b_i = \frac{L_w}{2} \sum_{l=0}^{\lceil \frac{L_w}{2\xi} \rceil - 1} (-1)^{\lfloor \frac{i+L_w-\xi}{\xi} \rfloor + l} w[m_i + l\xi] w[m_i + l\xi + \frac{L_w}{2}]. \quad (18)$$

a_i in (16) and b_i in (17) are periodic with period ξ while b_i in (18) is periodic with period 2ξ . We only have to compute them for one cycle.

For a given complex spectrogram $\mathbf{X} \in \mathbb{C}^{\frac{L_w}{2} \times \lceil \frac{L_x + L_w - \xi}{\xi} \rceil}$, define $\mathbf{y} := (y[0], y[1], \dots, y[L_x - 1])^T := \mathcal{S}^H(\mathbf{X})$. Then, the unique solution \mathbf{x} to a linear system $(\mathcal{S}^H \circ \mathcal{S}) \mathbf{x} = \mathbf{y}$ is the inversion result of \mathbf{X} . This linear system is decomposed into $\frac{L_w}{2}$ independent systems

$$\begin{bmatrix} a_0^{(i)} & b_0^{(i)} & & & \\ b_0^{(i)} & a_1^{(i)} & b_1^{(i)} & & \\ & \ddots & \ddots & \ddots & \\ & & b_{n_i-3}^{(i)} & a_{n_i-2}^{(i)} & b_{n_i-2}^{(i)} \\ & & & b_{n_i-2}^{(i)} & a_{n_i-1}^{(i)} \end{bmatrix} \begin{bmatrix} x[i] \\ x[i + \frac{L_w}{2}] \\ \vdots \\ x[i + \frac{(n_i-2)L_w}{2}] \\ x[i + \frac{(n_i-1)L_w}{2}] \end{bmatrix} = \begin{bmatrix} y[i] \\ y[i + \frac{L_w}{2}] \\ \vdots \\ y[i + \frac{(n_i-2)L_w}{2}] \\ y[i + \frac{(n_i-1)L_w}{2}] \end{bmatrix} \quad (19)$$

($i = 0, 1, \dots, \frac{L_w}{2} - 1$), where $n_i = \lceil \frac{2(L_x - i)}{L_w} \rceil$, $a_j^{(i)} := a_{i+j\frac{L_w}{2}}$ and $b_j^{(i)} := b_{i+j\frac{L_w}{2}}$. Since the matrices in the left side of (19) are *tridiagonal matrices*, their LU decompositions can be computed in $\mathcal{O}(n)$ [33], and the inversion result \mathbf{x} is also obtained from \mathbf{y} in $\mathcal{O}(n)$.¹⁰

In particular, when $\text{mod}_{\xi}(\frac{L_w}{2}) = 0$ for Type-I and Type-II, or $\text{mod}_{2\xi}(\frac{L_w}{2}) = 0$ for Type-III, we have $a_0^{(i)} = a_1^{(i)} = \dots = a_{n_i-1}^{(i)} = a_i$ and $b_0^{(i)} = b_1^{(i)} = \dots = b_{n_i-2}^{(i)} = b_i$, and hence the matrices in the left side of (19) are *tridiagonal Toeplitz matrices*. In such cases, the eigenvalues are $\lambda_q^{(i)} = a_i + 2b_i \cos(\frac{q\pi}{n_i+1}) > a_i - 2|b_i| > 0$ and the eigenvectors are $\mathbf{u}_q = (\sin(\frac{q\pi}{n_i+1}), \sin(\frac{2q\pi}{n_i+1}), \dots, \sin(\frac{n_i q\pi}{n_i+1}))^T \in \mathbb{R}^{n_i}$ ($q = 1, 2, \dots, n_i$) [34]. Therefore, the inversion result \mathbf{x} is also obtained by using the discrete sine transform (DST) of Type-I [35].

When $\text{mod}_{\xi}(\frac{L_w}{2}) = 0$ and $\text{mod}_{2\xi}(\frac{L_w}{2}) \neq 0$ for Type-III, we have $b_j^{(i)} = (-1)^j b_i$ for all i and j . We can also compute the inversion result \mathbf{x} by using Type-I DST, even in this case, with appropriate sign reversal process (see the actual program in [36] for more detail).

4.2. Inversion Based on the Pseudoinverse with the Periodicity

For Type-I and Type-II, let p be the minimum nonnegative integer s.t. $\text{mod}_{\frac{L_w}{2}}(\lceil \frac{L_x + L_w - \xi}{\xi} \rceil \xi + p\xi) = 0$. For Type-III, p must also satisfy $\text{mod}_{2\xi}(\lceil \frac{L_x + L_w - \xi}{\xi} \rceil \xi + p\xi) = 0$. We define $L_p := \lceil \frac{L_x + L_w - \xi}{\xi} \rceil \xi + p\xi$ and $\mathbf{x}_p := (x[0], x[1], \dots, x[L_x - 1], x[L_x], \dots, x[L_p - 1])^T := (\mathbf{x}^T, \mathbf{0}_{L_p - L_x}^T)^T \in \mathbb{C}^{L_p}$. Let $\mathcal{S}_p : \mathbb{C}^{L_p} \rightarrow \mathbb{C}^{\frac{L_w}{2} \times (\lceil \frac{L_x + L_w - \xi}{\xi} \rceil + p)}$ be a linear mapping, that computes one of (11), (12), and (13) for $l = 0, 1, \dots, \lceil \frac{L_x + L_w - 2\xi}{\xi} \rceil + p$ while assuming the *periodic condition*, i.e., $x[\tau] = x[L_p + \tau]$ for $\tau < 0$, according to the convention [6]–[8].

⁹Let $\mathbf{P}_l \in \mathbb{R}^{L_w \times L_x}$, $\mathbf{W} = \text{diag}(w[\tau]) \in \mathbb{R}^{L_w \times L_w}$, and $\mathbf{F}_u \in \mathbb{C}^{\frac{L_w}{2} \times L_w}$ be the l th frame extraction matrix, window matrix, and Type-I undersampled DFT matrix. We have $\mathcal{S}^H \circ \mathcal{S} = \sum_l \mathbf{P}_l^T \mathbf{W} \mathbf{F}_u^H \mathbf{F}_u \mathbf{W} \mathbf{P}_l$ for Type-I FUSTFT.

¹⁰The solver for tridiagonal systems is called the Thomas algorithm.

$$\begin{bmatrix} a_0^{(i)} b_0^{(i)} & & & b_{n_i-1}^{(i)} \\ b_0^{(i)} a_1^{(i)} & b_1^{(i)} & & \\ & \ddots & \ddots & \\ & & b_{n_i-3}^{(i)} a_{n_i-2}^{(i)} & b_{n_i-2}^{(i)} \\ & & & b_{n_i-2}^{(i)} a_{n_i-1}^{(i)} \\ b_{n_i-1}^{(i)} & & & \end{bmatrix} \begin{bmatrix} x[i] \\ x[i + \frac{L_w}{2}] \\ \vdots \\ x[i + \frac{(n_i-2)L_w}{2}] \\ x[i + \frac{(n_i-1)L_w}{2}] \end{bmatrix} = \begin{bmatrix} y[i] \\ y[i + \frac{L_w}{2}] \\ \vdots \\ y[i + \frac{(n_i-2)L_w}{2}] \\ y[i + \frac{(n_i-1)L_w}{2}] \end{bmatrix} \quad (20)$$

¹⁸In Tables 1 and 2, we call $\|\cdot\|_{\mathbb{F}}^{\text{int}}$ the *interior* Frobenius norm that ignores components in the first $\lceil \frac{L_w - \xi}{\xi} \rceil$ and last $\lceil \frac{L_x + L_w - \xi}{\xi} \rceil - \frac{L_x}{\xi}$ time frames.

6. REFERENCES

- [1] M. R. Portnoff, "Implementation of the digital phase vocoder using the fast Fourier transform," *IEEE Trans. Acoust. Speech Signal Process.*, vol. 24, no. 3, pp. 243–248, 1976.
- [2] J. B. Allen, "Short term spectral analysis, synthesis, and modification by discrete Fourier transform," *IEEE Trans. Acoust. Speech Signal Process.*, vol. 25, no. 3, pp. 235–238, 1977.
- [3] J. B. Allen and L. R. Rabiner, "A unified approach to short-time Fourier analysis and synthesis," *Proc. IEEE*, vol. 65, no. 11, pp. 1558–1564, 1977.
- [4] R. E. Crochiere, "A weighted overlap-add method of short-time Fourier analysis/synthesis," *IEEE Trans. Acoust. Speech Signal Process.*, vol. 28, no. 1, pp. 99–102, 1980.
- [5] L. Cohen, *Time-Frequency Analysis: Theory and Applications*. Englewood Cliffs, NJ: Prentice Hall, 1994.
- [6] H. G. Feichtinger and T. Strohmer, Eds., *Gabor Analysis and Algorithms: Theory and Applications*. Secaucus, NJ: Birkhäuser, 1997.
- [7] K. Gröchenig, *Foundations of Time-Frequency Analysis*. Secaucus, NJ: Birkhäuser, 2001.
- [8] H. G. Feichtinger and T. Strohmer, Eds., *Advances in Gabor Analysis*. Secaucus, NJ: Birkhäuser, 2002.
- [9] P. L. Søndergaard, "Finite discrete Gabor analysis," *Ph.D. thesis*, Technical University of Denmark, 2007.
- [10] K. Yatabe, Y. Masuyama, T. Kusano, and Y. Oikawa, "Representation of complex spectrogram via phase conversion," *Acoust. Sci. & Tech.*, vol. 40, no. 3, pp. 170–177, 2019.
- [11] H. S. Malvar, "Lapped transforms for efficient transform/sub-band coding," *IEEE Trans. Acoust. Speech Signal Process.*, vol. 38, no. 6, pp. 969–978, 1990.
- [12] I. Daubechies, S. Jaffard and J. Journé, "A simple Wilson orthonormal basis with exponential decay," *SIAM J. Math. Anal.*, vol. 22, no. 2, pp. 554–573, 1991.
- [13] H. Bölcskei, G. Feichtinger, K. Gröchenig, and F. Hlawatsch, "Discrete-time Wilson expansions," in *Proc. TFTS*, Paris, 1996, pp. 525–528.
- [14] H. S. Malvar, "A modulated complex lapped transform and its applications to audio processing," in *Proc. ICASSP*, Phoenix, AZ, 1999, pp. 1421–1424.
- [15] J. C. Brown, "Calculation of a constant-Q spectral transform," *J. Acoust. Soc. Am.*, vol. 89, no. 1, pp. 425–434, 1991.
- [16] I. Daubechies, *Ten Lectures on Wavelets*, ser. CBMS-NSF Regional Conference Series in Applied Mathematics. Philadelphia, PA: SIAM, 1992, vol. 61.
- [17] J. J. Benedetto and M. W. Frazier, *Wavelets: Mathematics and Applications*, ser. Studies in Advanced Mathematics. Boca Raton, FL: CRC Press, 1993, vol. 13.
- [18] G. Kaiser, *A Friendly Guide to Wavelets*. Secaucus, NJ: Birkhäuser, 2011.
- [19] V. Verfaillie, U. Zolzer, and D. Arfib, "Adaptive digital audio effects (A-DAFx): A new class of sound transformations," *IEEE Transactions on Audio, Speech, and Language Processing*, vol. 14, no. 5, pp. 1817–1831, 2006.
- [20] G. Yu, S. Mallat, and E. Bacry, "Audio denoising by time-frequency block thresholding," *IEEE Trans. on Signal Process.*, vol. 56, no. 5, pp. 1830–1839, 2008.
- [21] E. Benetos, S. Dixon, D. Giannoulis, H. Kirchhoff, and A. Klauri, "Automatic music transcription: challenges and future directions," *J. Intel. Inf. Syst.*, vol. 41, no. 3, pp. 407–434, 2013.
- [22] M. Mauch, C. Cannam, R. Bittner, G. Fazekas, J. Salamon, J. Dai, J. Bello, and S. Dixon, "Computer-aided melody note transcription using the Tony software: accuracy and efficiency," in *Proc. TENOR*, Paris, 2015, pp. 28–30.
- [23] T. Fujiwara, M. Yamagishi, and I. Yamada, "Reduced-rank modeling of time-varying spectral patterns for supervised source separation," in *Proc. ICASSP*, Brisbane, 2015, pp. 3307–3311.
- [24] Y. Wakabayashi and N. Ono, "Griffin-Lim phase reconstruction using short-time Fourier transform with zero-padded frame analysis," in *Proc. APSIPA ASC*, Lanzhou, 2019, pp. 1863–1867.
- [25] Y. Takahashi, D. Kitahara, K. Matsuura, and A. Hirabayashi, "Determined source separation using the sparsity of impulse responses," in *Proc. ICASSP*, Barcelona, 2020, pp. 686–690.
- [26] R. Nakatsu, D. Kitahara, and A. Hirabayashi, "Non-Griffin-Lim type signal recovery from magnitude spectrogram," in *Proc. ICASSP*, Barcelona, 2020, pp. 791–795.
- [27] T. Werther, Y. C. Eldar, and N. K. Subbanna, "Dual Gabor frames: theory and computational aspects," *IEEE Trans. Signal Process.*, vol. 53, no. 11, pp. 4147–4158, 2005.
- [28] B. Yang, "A study of inverse short-time Fourier transform," in *Proc. ICASSP*, Las Vegas, NV, 2008, pp. 3541–3544.
- [29] I. Daubechies, A. Grossmann, and Y. Meyer, "Painless nonorthogonal expansions," *J. Math. Phys.*, vol. 27, no. 5, pp. 1271–1283, 1986.
- [30] L. Stanković, "On the STFT inversion redundancy," *IEEE Trans. Circuits Syst. II: Express Briefs*, vol. 63, no. 3, pp. 284–288, 2016.
- [31] S. Moreno-Picot, F. J. Ferri, M. Arevalillo-Herráez, and W. Díaz-Villanueva, "Efficient analysis and synthesis using a new factorization of the Gabor frame matrix," *IEEE Trans. Signal Process.*, vol. 66, no. 17, pp. 4564–4573, 2018.
- [32] MathWorks, "Modified discrete cosine transform: MATLAB mdct." <https://www.mathworks.com/help/audio/ref/mdct.html>
- [33] L. H. Thomas, "Elliptic problems in linear differential equations over a network," *Watson Sci. Comput. Lab. Report*, Columbia Univ., 1949.
- [34] S. Noschese, L. Pasquini, and L. Reichel, "Tridiagonal Toeplitz matrices: properties and novel applications," *Numer. Linear Algebra Appl.*, vol. 20, no. 2, pp. 302–326, 2013.
- [35] S. A. Martucci, "Symmetric convolution and the discrete sine and cosine transforms," *IEEE Trans. Signal Process.*, vol. 42, no. 5, pp. 1038–1051, 1994.
- [36] D. Kitahara, The MATLAB program of FUSTFT, <https://lab.d-kitahara.com/codes/>
- [37] M. M. Chawla and R. R. Khazal, "A parallel elimination method for "periodic" tridiagonal systems," *Int. J. Comput. Math.*, vol. 79, no. 4, pp. 473–484, 2002.